SLAC-PUB-17151

X-RAY REGENERATIVE AMPLIFIER FREE-ELECTRON LASER CONCEPTS FOR LCLS-II

G. Marcus, Y. Ding, J. Duris, Y. Feng, Z. Huang, J. Krzywinski, T. Maxwell, D. Ratner,
T. Raubenheimer, SLAC, Menlo Park, USA
K.-J. Kim, R. Lindberg, Y. Shvyd'ko, ANL, Argonne, USA
D. Nguyen, LANL, Los Alamos, USA

Abstract

High brightness electron beams that will drive the next generation of high repetition rate X-ray FELs allow for the possibility of optical cavity based feedback. One such cavity based FEL concept is the Regenerative Amplifier Free-Electron Laser (RAFEL). This paper examines the design and performance of possible RAFEL configurations for LCLS-II. The results are primarily based on high-fidelity numerical particle simulations that show the production of high brightness, high average power, fully coherent, and stable X-ray pulses at LCLS-II using both the fundamental and harmonic FEL interactions.

INTRODUCTION

XFELs such as the LCLS, based primarily on Self-Amplified Spontaneous Emission (SASE), are capable of producing extremely bright, transversally coherent, ultra-short pulses suitable for the investigation of ultra-fast chemical and physical processes that operate on the time and length scales of atomic and molecular motion [1, 2]. A characteristic feature of single-pass SASE FELs, however, is poor longitudinal coherence, which results from the initial amplification of incoherent radiation shot-noise [3, 4]. Improvement of the longitudinal coherence is of great practical importance and has been the subject of many recent investigations. Longitudinal coherence can be obtained by seeding the FEL amplifier with sufficiently narrow bandwidth radiation well above the effective shot noise power in the electron beam. Examples of this include self-seeding [5], which has been successfully implemented at LCLS in both the hard [6] and soft X-ray [7] spectral regimes and externally seeded schemes, which are currently being vetted as possible upgrade paths for LCLS-II soft X-rays [8]. Self-seeding, however, nominally suffers from low seed power in an attempt to preserve the electron beam properties important for lasing and is fundamentally still dependent on the noisy SASE process leading to large (100%) seed power fluctuations. External seeding necessarily requires high-harmonic conversions that have inherent challenges [9]. The RAFEL concept, studied here, offers an alternative pathway to the production of stable, fully coherent, high brightness, and high average power X-ray radiation.

Similar to an XFEL oscillator [10], a RAFEL consists of a high repetition rate electron beam, a short undulator and an X-ray crystal cavity (in the case of hard X-rays) to provide optical feedback (see, for example, Fig. 1). However, unlike an oscillator, which operates as a low-gain FEL in a low output coupling cavity, the RAFEL is a high-gain FEL that reaches saturation in only a few round trips in a high output coupling cavity. The RAFEL concept exhibits many additional distinct advantages over an oscillator when considering challenges associated with potential cavity design. The high-gain FEL should be less sensitive to X-ray induced cavity optics degradation and the small number of cavity passes should relax the longitudinal alignment tolerances relative to what is expected with an oscillator cavity. In addition, the RAFEL cavity does not serve the function of defining the transverse radiation mode since the dominant amplified mode is gain guided. This substantially relaxes the cavity opto-mechanical stability and crystal positioning requirements. The main responsibility of the cavity is to recirculate the radiation, which, in turn, seeds successive electron bunches . This optical feedback also allows for a reduced undulator length relative to SASE and can ultimately produce longitudinally coherent X-ray pulses close to the Fourier Transform limit.

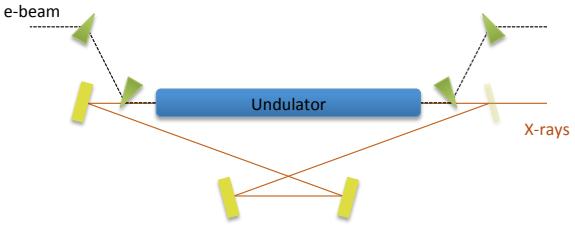

Figure 1: RAFEL concept where the X-ray cavity is wrapped around the entire undulator.

This paper reports the results of preliminary RAFEL studies within the context of the LCLS-II project. Numerical particle simulations using the FEL code `GENESIS` [11] are used to explore, in an ideal sense, possible RAFEL performance at LCLS-II in both the soft and hard X-ray spectral regimes. Results from lasing at both the fundamental FEL resonance wavelength as well as harmonics, using harmonic lasing [12–14], are presented.

SIMULATION STRATEGY

The high repetition rate LCLS-II FEL has been thoroughly studied and the challenges associated with generating, accelerating, and transporting high brightness electron beams to the undulators are well understood and documented (e.g. see [15–17] and references therein). Global optimizations of the electron beam delivery system and SASE FEL performance for charge distributions that span the planned opera-

This material is based upon work supported by the U.S. Department of Energy, Office of Science, under Contract No. DE-AC02-76SF00515.

tional range are ongoing. However, seeded FELs can suffer from pedestal growth caused by microbunching-instability induced energy and density modulations on the electron beam [18]. Running hundreds to thousands of full start-to-end simulations in order to capture these effects for a single RAFEL simulation is untenable. Therefore, the start-to-end simulations were used to define the slice properties of an ideal electron beam that was used in the FEL simulations. The electron beams used in the simulations below had a flat-top current profile and gaussian distributions in energy as well as the transverse dimensions.

Electron beams both with and without the effects of the space charge driven microbunching-instability are included below where only energy modulations on the beam longitudinal profile are included. For simulations with microbunching modulations, the spectrum of the energy structure is modeled to mimic the general microbunching gain spectrum due to longitudinal space charge and has the form

$$p_0 = p + C\sum_i^N \left(\frac{\lambda_0}{\lambda_i}\right)^2 \exp\left(\left(\frac{\lambda_0}{\lambda_i}\right)^2\right)\sin\left(\frac{2\pi}{\lambda_i}s + \phi_i\right), \quad (1)$$

where p is the momentum, N is the number of individual modulations (typically around 100), λ_0 is the peak wavelength of the microbunching spectrum (here around $2\mu m$), λ_i is a particular microbunching wavelength within the spectral envelope, ϕ is a random phase, and C is an amplitude chosen to adjust the integrated energy spread.

Optical cavity design challenges and constraints, which can be significant, are not considered here. As such, optical propagation through potential cavity geometries was not considered in the simulations, although implementation would be straightforward [19]. The fields are assumed to be re-imaged at the entrance to the undulator in the transverse planes while the various cavity detunings that were studied served to shift the field in time with respect to the arrival of the electrons.

HXR SIMULATION RESULTS

Harmonic lasing was used in order to both increase the performance at the high end of the hard X-ray undulator tuning range (5 keV) and to extend the photon energy reach beyond this limit (9 keV). We present the results from simulation below.

5 keV

The results of high-fidelity start-to-end simulations for the low charge (20 pC) operational mode at LCLS-II were used to define the slice properties of the ideal electron beam that were used in the HXR RAFEL simulations. The slice properties as well as the undulator parameters used for this study can be found in Table 1. For simplicity, the nominal LCLS-II undulator parameters are used here. The X-ray crystal Bragg mirrors that would nominally compose the recirculating optical cavity would provide some frequency filtering due to their limited reflectivity bandwidth [20]. This is modeled in a very simple way here where a Gaussian filter with resolving power $R = 15,000$ is used to model a reflectivity curve and is applied once before interaction with a fresh electron beam. This filter is also used to model the high output coupling associated with a RAFEL cavity by returning only 10% of the FEL power per round trip. It should be noted that the bandwidth and reflectivity associated with this filter is much larger and less efficient than typical Bragg mirrors. However, it was useful to use these parameters to establish and learn about the RAFEL output dependencies on the various knobs available (gain length, undulator length, cavity detuning, output coupling, etc.). The results of 10 passes through the RAFEL system are shown in Fig. 2, which compares the spectrum of the RAFEL tuned to produce 5 keV radiation at the 3rd harmonic to SASE at the fundamental. Preliminary simulations show that a RAFEL can increase the peak spectral brightness of the baseline LCLS-II performance at 5 keV by greater than a factor of 20 at saturation (the electron

Table 1: Nominal 20(100) pC Electron Beam and Undulator Parameters for the Baseline LCLS-II Scenario.

Paramter	Symbol	Value	Unit
e-beam energy	E	4.0	GeV
emittance	ϵ	0.15(0.4)	μm
current	I	0.5(1)	kA
energy spread	σ_E	400	keV
beta	$\langle\beta\rangle$	15	m
undulator period	λ_u	26(39)	mm
segment length	L_u	3.4	m
break length	L_b	1.0	m

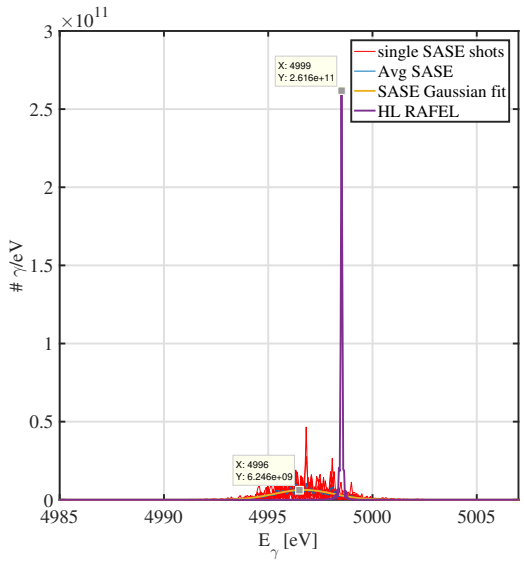

Figure 2: Comparison of the spectral brightness at 5 keV from SASE at the fundamental resonant wavelength to the RAFEL using the 3rd harmonic.

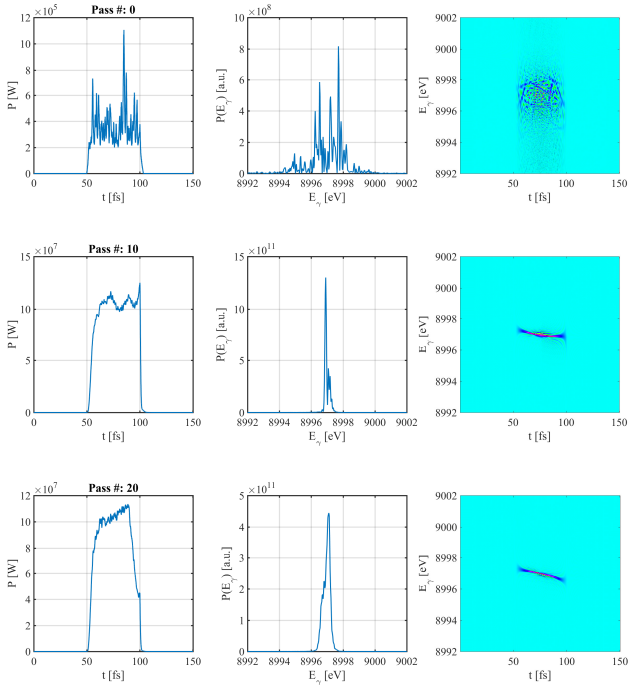

Figure 3: Results for 3rd harmonic lasing at 9 keV in the RAFEL for three passes starting from noise.Top row: pass 0. Middle row: pass 10. Bottom row: pass 20. The first column is the temporal profile of the radiation at the exit of the undulator, the second column is the spectrum and the third column is the Wigner profile.

beam used in the RAFEL simulations was twice as long as the beam used in SASE simulations).

9 keV

The procedure for frequency and amplitude filtering described above is used to investigate the possibility of using a RAFEL at the 3rd harmonic to produce radiation far above the nominal reach of SASE at the fundamental using the 4.0 GeV energy LCLS-II electron beam. Figure 3 shows the results, after optimizing the cavity detuning and undulator length for a 90% output coupling, at various passes during the RAFEL amplification starting from noise. Full three-dimensional coherence is reached with significant power after only 20 passes.

SXR SIMULATION RESULTS

Much progress is being made in the development of high quality optics in the soft X-ray spectral range [21]. While the demonstration of optics possessing the properties necessary for a RAFEL optical cavity are probably far off, it is still instructive to establish a baseline performance to compare against other seeding techniques [8]. To this end, the RAFEL performance at a 1 nm resonance wavelength and 90% output coupling was investigated using the fundamental FEL interaction for LCLS-II like parameters. The ideal electron beam used in these simulations was defined using the slice

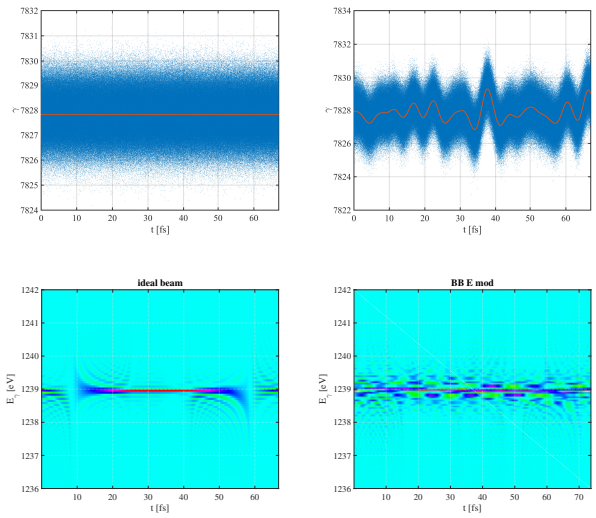

Figure 4: Longitudinal phase space of a typical ideal electron beam (top left) and an electron beam with broadband energy modulations (top right) used in simulation. Below are the corresponding normalized on-axis Wigner distributions of the X-rays after 100 passes (bottom left) and 145 passes (bottom right).

properties of a typical 100 pC start-to-end beam, which can be found in Table 1. Along with these ideal simulations, as mentioned above, the microbunching induced energy modulations that are reflected in typical start-to-end beams are modeled to investigate their effect on the spectral properties of the RAFEL output.

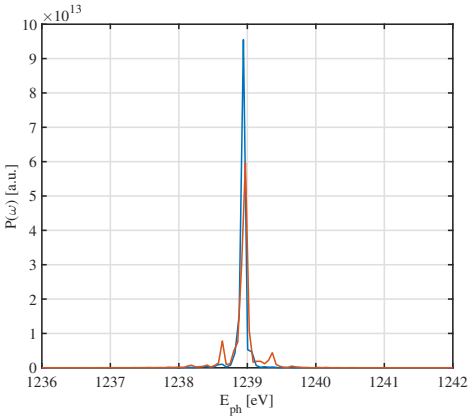

Figure 5: Spectral comparison for a 1 nm RAFEL driven by an ideal electron beam (blue) and an electron beam with broadband energy modulations (red).

1 nm

Figure 4 shows the longitudinal phase space of electron beams that have been used in simulation to investigate the RAFEL performance at 1 nm as well as the Wigner distributions of the amplified light after 100 passes (ideal electron

beam, left) and 145 passes (broadband energy modulations, right).

While the ideal electron beam produces light with full longitudinal coherence, the broadband energy modulations create some structure on the pulse. This is clearly seen as the amplification of sidebands in Fig. 5, which shows a spectral comparison between the two scenarios.

The peak spectral brightness, however, does not suffer significantly and compares well with other externally seeded scenarios [8]. It should be noted that no spectral filtering has been applied in these cases. The FEL, which is a group-velocity dispersion medium, cleans up the spectrum through continuous slippage. The cavity detuning and undulator length have to be carefully chosen to keep the amplification in the exponential gain regime just up to saturation and to allow the phase information to be propagated from the back of the beam forward over many passes.

CONCLUSION

Preliminary simulations show that various RAFEL configurations can boost the performance of the LCLS-II at the high end of the tuning range in the HXR undulator, can extend the tuning range far beyond the nominal 5 keV limit, and compare well with externally seeded schemes in the SXR spectral range at the high end of the tuning range. Harmonic lasing, which works well with seeded schemes as opposed to the more difficult SASE case, can be leveraged in many cases. Detailed optical cavity designs, as well as their associated challenges, have not been considered here but are an ongoing effort. The performance boost experienced in the SXR spectral range relative to externally seeded schemes could potentially warrant additional investigations into optics suitable for a RAFEL cavity where current limitations, including being limited to large angle, or grazing incidence, reflections, and inefficient and narrow reflectivity bandwidth, are prohibitive.

ACKNOWLEDGMENT

This work was supported by the U.S. Department of Energy under contract No. DE-AC02-76SF00515.

REFERENCES

[1] P. Emma *et al.*, "First lasing and operation of an Ångstrom-wavelength free-electron laser", *Nature Photonics* vol. 4, no. 641, 2010.

[2] C. Bostedt *et al.*, "Ultra-fast and ultra-intense x-ray sciences: first results from the Linac Coherent Light Source free-electron laser", *Journal of Physics B: Atomic, Molecular and Optical Physics*, vol. 46, no. 16, p. 164003, 2013.

[3] R. Bonifacio, C. Pellegrini, and L. M. Narducci, "Collective instabilities and high-gain regime in a free electron laser", *Opt. Commun.*, vol. 50, no. 373, 1984.

[4] R. Bonifacio, L. De Salvo, P. Pierini, N. Piovella, and C. Pellegrini, "Spectrum, temporal structure, and fluctuations in a high-gain free-electron laser starting from noise", *Phys. Rev. Lett.*, vol. 73, no. 70, 1994.

[5] J. Feldhaus, E. Saldin, J. Schneider, E. Schneidmiller, and M. Yurkov, "Possible application of x-ray optical elements for reducing he spectral bandwidth of an x-ray SASE FEL", *Opt. Commun.*, vol. 140, no. 341, 1997.

[6] J. Amann *et al.*, "Demonstration of self-seeding in a hard-x-ray free-electron laser", *Nature Photonics*, vol. 6, no. 693, 2012.

[7] D. Ratner *et al.*, "Experimental demonstration of a soft x-ray self-seeded free-electron laser", *Phys. Rev. Lett.*, vol. 114, p. 054801, 2015.

[8] E. Hemsing, "Seeding experiments and seeding options for LCLS II", presented at FEL'17, New Mexico, USA, paper TUB01, this conference.

[9] E. Allaria *et al.*, "Two-stage seeded soft-x-ray free-electron laser", *Nature Photonics*, vol. 7, no. 913, 2013.

[10] K.-J. Kim, Y. Shvyd'ko, and Sven Reiche, "A proposal for an x-ray free-electron laser oscillator with an energy-recovery linac", *Phys. Rev. Lett.*, vol. 100, p. 244802, 2008.

[11] S. Reiche, "GENESIS 1.3: a fully 3D time-dependent FEL simulation code", *Nucl. Instr. Meth. Phys. Res. Sect. A*, vol. 429, p. 243, 1999.

[12] B. W. J. McNeil, G. R. M. Robb, M. W. Poole, and N. R. Thompson, "Harmonic lasing in a free-electron-laser amplifier", *Phys. Rev. Lett*, vol. 96, p. 084801, 2006.

[13] E. A. Schneidmiller and M.V. Yurkov, "Harmonic lasing in x-ray free electron lasers", *Phys. Rev. ST Accel. Beams*, vol. 15, p. 080702, 2012.

[14] G. Marcus, Y. Ding, Z. Huang, T.O. Raubenheimer, and G. Penn, "Harmonic lasing options for LCLS-II", in *Proceedings of the 36th International Free Electron Laser Conference*, Basel, Switzerland, August 2014, paper MOP054, pp. 148-152.

[15] G. Marcus *et al.*, "High fidelity start-to-end numerical particle simulations and performance studies for LCLS-II", in *Proceedings of the 37th International Free Electron Laser Conference*, Daejeon, Korea, August 2015, paper TUP007, pp. 342-346.

[16] J. Qiang *et al.*, "Start-to-end simulation of the LCLS-II beam delivery system with real number of electrons", in *Proceedings of the 37th International Free Electron Laser Conference*, Daejeon, Korea, August 2015, paper WEP070, pp. 714-717.

[17] T.O. Raubenheimer, "LCLS-II: Status of the CW x-ray FEL upgrade to the SLAC LCLS facility", in *Proceedings of the 37th International Free Electron Laser Conference*, Daejeon, Korea, August 2015, paper WEP014, pp. 618-624.

[18] Z. Zhang *et al.*, "Microbunching-instability-induced sidebands in a seeded free-electron laser", *Phys. Rev. Accel. Beams*, vol. 19, p. 050701, 2016.

[19] G. Marcus "Spatial and temporal pulse propagation for dispersive paraxial optical systems", *Optics Express*, vol. 24, p. 7752, 2016.

[20] Z. Huang and R.D. Ruth, "Fully coherent x-ray pulses from a regenerative-amplifier free-electron laser", *Phys. Rev. Lett.*, vol. 96, p. 144801, 2006.

[21] N. Ghafoor *et al.*, "Impact of B_4C co-sputtering on structure and optical performance of Cr/Sc multilayer x-ray mirrors", *Optics Express*, vol. 25, p. 18274, 2017.